Anti-tubercular activity of novel 4-anilinoquinolines and 4-anilinoquinazolines

Christopher R. M. Asquith[a,b], Neil Fleck[c], Christoph Grundner[c,d,*], William J. Zuercher[b,e,*]

[a]*Department of Pharmacology, School of Medicine University of North Carolina at Chapel Hill, Chapel Hill, NC 27599, USA*
[b]*Structural Genomics Consortium, UNC Eshelman School of Pharmacy, University of North Carolina at Chapel Hill, Chapel Hill, NC, 27599, USA*
[c]*Seattle Children's Research Institute, Seattle, Washington, 98101, USA*
[d]*Department of Global Health, University of Washington, Seattle, Washington, 98195, USA*
[e]*Lineberger Comprehensive Cancer Center, University of North Carolina at Chapel Hill, Chapel Hill, NC 27599, USA*

ARTICLE INFO

Article history:
Received
Revised
Accepted
Available online

Keywords:
Anti-tubercular
4-anilinoquinoline
4-anilinoquinazoline
Mycobacterium tuberculosis (*Mtb*)

ABSTRACT

We screened a series of 4-anilinoquinolines and 4-anilinoquinazolines and identified novel inhibitors of *Mycobacterium tuberculosis* (*Mtb*). The focused 4-anilinoquinoline/quinazoline scaffold arrays yielded compounds with high potency and the identification of 6,7-dimethoxy-*N*-(4-((4-methylbenzyl)oxy)phenyl)quinolin-4-amine (**34**) with an MIC_{99} value of 1.25-2.5 µM. We also define a series of key structural features including the benzyloxy aniline and the 6,7-dimethoxy quinoline ring that are important for *Mtb* inhibition.

Mycobacterium tuberculosis (*Mtb*), the causative agent of tuberculosis (TB) in humans,[1] infects nearly a third of the earth's population and caused 1.6 million worldwide deaths in 2017.[2] With nearly ten million new cases of active disease each year, TB is now the leading cause of death from infectious disease globally.[2] Current therapeutic strategies involve the use of a combination of anti-microbial agents including ethambutol, isoniazid, pyrazinamide and rifampicin (fig. 1).[3] However, more than 5% of *Mtb* infections now involve multidrug-resistant (MDR-TB) and extensively drug-resistant (XDR-TB) *Mtb* strains. MDR-TB is

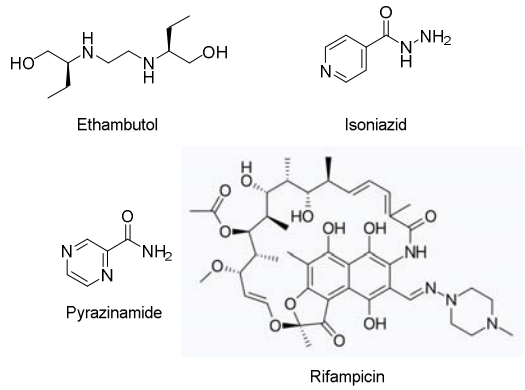

Figure 1. Current therapeutic strategies for treatment of *Mycobacterium tuberculosis* infections.

associated with a 50% mortality rate whereas XDR-TB is nearly always fatal.[4] There is an urgent need for new therapeutic strategies.

Human protein kinases are pharmacologically tractable enzymes targeted by more than three dozen approved medicines.[5] Hundreds of additional kinase inhibitors are under clinical and preclinical investigation. There is growing recognition that pathogen kinases may be targeted in the treatment of infectious diseases.[6-7] Considering the conserved ATP-binding site across species, we looked to screen collections of ATP-competitive inhibitors of human kinases for their anti-tubercular activity.

There have been several efforts to map the ATP-competitive inhibitor landscape, notably with the first- and second-generation GlaxoSmithKline Published Kinase Inhibitor Sets (PKIS and PKIS2), collections of well characterized ATP-competitive kinase inhibitors with broad coverage of the human kinome.[8-9] These sets and wider inhibitor screening efforts have found utility in identifying inhibitors of additional human kinases as well as kinases from other organisms, both eukaryotic and prokaryotic.[10-14]

To identify new chemical starting points against *Mtb* we looked to lapatinib, gefitinib, and erlotinib as starting points which have recently been revealed to have activity against Mtb (Fig. 2.).[5,15] We tested the activity of lapatinib, gefitinib, and erlotinib against *Mtb* by measuring luminescence and growth on solid medium across a series of compound concentrations (20 – 0.625 µM) (Tab 2).[16-17] The reduction of visible growth on solid medium demonstrated the compounds to be bactericidal.

Gefitinib treatment had no effect relative to the absence of compound. Erlotinib induced a modest effect that appeared to plateau at a signal of approximately 70 %. In contrast, lapatinib showed activity even at 5 µM and reduced the relative *Mtb* signal to below 10 % at 20 µM. This result suggested that the 4-benzyloxy aniline substituent might be important for anti-Mtb activity.

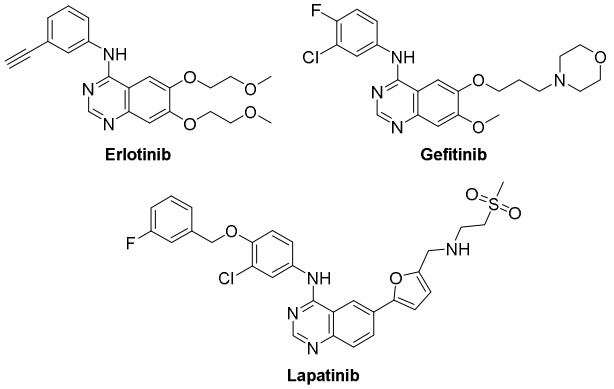

Figure 2. Structures of clinical quinazolines.

Table 1. Result of clinical inhibitors

Compound /µM	*Mtb* signal[a]				
	1.25	**2.5**	**5**	**10**	**20**
Gefitinib	1.08	1.09	1.05	1.08	1.05
Erlotinib	1.05	0.96	0.9	0.68	0.7
Lapatinib	0.99	0.9	0.74	0.17	0.08

[a]Relative luminescence measured at 3 days after treatment. Values = RLU(sample)/RLU(no compound) at µM concentrations and no effect at 0.625 µM

To further explore quinazoline *Mtb* activity, we profiled several focused arrays of compounds to probe the structure activity relationships of the quinoline/quinazoline. We hence synthesized a series of compounds (**1**-**34**) following up on GW320571X, a PKIS2 quinazoline, through nucleophilic aromatic displacement of 4-chloroquin(az)olines. (Scheme 1) We were able to access products in good to excellent yields (55-91 %) consistent with previous reports and without protection of the alcohol substituted quin(az)oline starting material.[10,18]

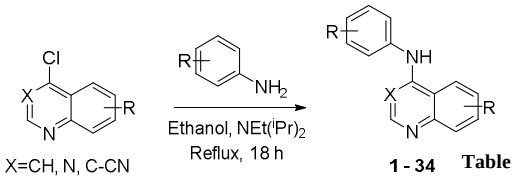

Scheme 1. General synthetic procedure

The first set of compounds probed a replacement of the 6-postion morpholine segment of gefitinib with a simple alcohol (Tab. 2).[20] Although neither the 6-OH (**1**) or 7-OH (**2**) quinazoline showed appreciable activity, the 6,7-dihydroxy compound (**3**) began to inhibit *Mtb* growth at higher concentrations. The analogous set of methoxy-substituted compounds (**4**-**6**) had very similar activity profiles. The 6-OH quinoline (**7**) showed improved activity relative to the matched quinazoline (**1**). The inclusion of fluorine substitution on the phenyl ring distal to the quinazoline (**8**-**10**) led to markedly increased activity for all three isomers. At 20 µM, **8**-**10** all reduced the relative *Mtb* signal to 25-37 %, and a modest but discernable reduction in signal was observed at 1.25 µM. Interestingly, the effect of fluorine substitution led to a different activity pattern from changing quinazoline ring substitution as the modification of **1** to the 7-OH (**11**) or 6,7-$(OH)_2$ (**12**) resulted in a significant loss of activity, even at 20 µM. These results demonstrated that *Mtb* activity was sensitive to changes at multiple parts of the template and that these changes were not necessarily additive.

The next set of quin(az)olines profiled was prepared to explore the contributions from both the aniline and the core heterocycle (Tab. 3).[18,21] The larger 3,4,5-trimethoxyphenyl aniline was employed on several diversely substituted quinolines and

Table 2. Results of alcohol replacement of the imidazole of GW320571X (**1**-**12**)

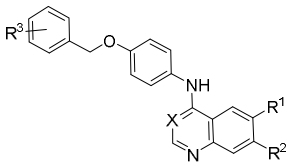

Compound	X	R^1	R^2	R^3	*Mtb* signal[a]				
					1.25 µM	**2.5 µM**	**5 µM**	**10 µM**	**20 µM**
1	N	OH	H	H	0.95	0.94	0.96	0.90	0.80
2	N	H	OH	H	0.90	0.90	0.89	0.88	0.89
3	N	OH	OH	H	0.95	0.93	0.91	0.76	0.69
4	N	OMe	H	H	1.04	1.07	0.89	0.83	0.62
5	N	H	OMe	H	1.05	1.12	0.99	0.87	0.64
6	N	OMe	OMe	H	1.04	1.04	0.83	0.77	0.60
7	CH	OH	H	H	0.95	0.86	0.66	0.42	0.37
8	N	OH	H	4-F	0.86	0.76	0.64	0.44	0.32
9	N	OH	H	3-F	0.76	0.64	0.49	0.39	0.25
10	N	OH	H	2-F	0.89	0.82	0.63	0.46	0.28
11	N	H	OH	4-F	0.94	1.01	0.90	0.89	0.83
12	N	OH	OH	4-F	1.04	1.14	1.00	0.89	0.76

[a]Relative luminescence measured at 3 days after treatment. Values = RLU(sample)/RLU(no compound) at µM concentrations and no effect at 0.625 µM

Table 3. Matched pair comparison of structures similar to erlotinib and lapatinib (**13**-**28**)

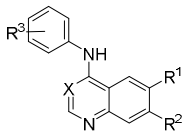

Compound	R^1	R^2	X	R^3	*Mtb* signal[a,b]

					5 µM	10 µM	20 µM
13	CF_3	H	CH	3,4,5-$(OMe)_3$	1.23	1.14	1.21
14	CF_3	H	N	3,4,5-$(OMe)_3$	1.25	1.12	1.06
15	Br	H	CH	3,4,5-$(OMe)_3$	1.35	1.41	1.28
16	OMe	OMe	CH	3,4,5-$(OMe)_3$	1.26	1.11	1.06
17	OMe	OMe	N	3,4,5-$(OMe)_3$	1.03	1.01	0.94
18	OMe	OMe	CN	3,4,5-$(OMe)_3$	1.03	1.01	0.97
19	6,7-$(OCH_2CH_2OMe)_2$		N	3,4,5-$(OMe)_3$	1.02	0.96	0.87
20	6,7-$(OCH_2CH_2OMe)_2$		CH	3-Ethynyl	0.88	0.79	0.58
21	OMe	OMe	CH	3-Ethynyl	1.02	0.89	0.67
22	OMe	OMe	N	3-Ethynyl	0.93	0.83	0.69
23	OMe	OMe	CN	3-Ethynyl	1.08	1.03	0.98
24	OMe	OMe	CH	3-Bromo	1.03	0.9	0.6
25	OMe	OMe	N	3-Bromo	0.98	0.71	0.65
26	OMe	OMe	CN	3-Bromo	0.88	0.56	0.37
27	OMe	OMe	N	3-Cl-4-(2-F-PhO)	0.92	0.74	0.8
28	OMe	OMe	CH	3-Cl-4-(2-F-PhO)	0.78	0.22	0.1

[a]Relative luminescence was measured at 3 days after treatment. Values = RLU(sample)/RLU(no compound); [b]None of the compounds reduced the relative *Mtb* signal below 95 % at 1.3 or 2.5 µM.

quinazolines (**13**-**18**) which led to no observable activity except when paired with the 6,7-$(OCH_2CH_2OMe)_2$-quinazoline of erlotinib (**19**) which had only slight activity at 20 µM. On the other hand, incorporation of the aniline fragment from erlotinib (3-ethynylphenyl) did yield several active compounds, including the quinoline analog of erlotinib (**20**). The erlotinib aniline with a 6,7-$(OMe)_2$-substituted quinoline core (**21**) or quinazoline (**22**) showed activity but not with the 3-cyanoquinoline (**23**). The analogous 3-bromophenyl aniline compounds (**24**-**26**) showed higher activity than the paired 3-ethynylphenyl compounds. Finally, the aniline substitution from lapatinib (3-Cl-4-(2-F-PhO)Ph) yielded a marginally active quinazoline (**27**) and a highly active quinoline (**28**) that had 10 % *Mtb* signal at 20 µM.

A final small set of compounds explored features of the 4-benzyloxyaniline portion of the quinoline template (Tab. 4).[22] Variation of the ether linkage to an amide and addition of a hydroxy on the aniline portion revealed an activity pattern where 6,7-dimethoxy substitution with the benzylic arm was active (**29**-**30**). In contrast, truncation of the benzyl also removed the activity as in acetamide **31** with no effect on *Mtb*. The mono-substituted 6-methoxy (**32**) and 7-methoxy (**33**) showed no reduction in *Mtb* signal at 20 µM. However, switching back to the 4-methyl benzyl ether linked compound **34** yielded the highest activity observed with any compound in the present study, with a robust signal observed even at 1.25 µM. The *Mtb* MIC_{99} for **34** was in the 1.25-2.5 µM range (Fig. 3).

These results define a series of structure activity relationships between *Mtb* activity and the 4-anilinoquinoline/quinazoline scaffold that could be used to inform a medicinal chemistry, trajectory for enhanced *Mtb* activity. The most sensitive structural changes were found to be in the ring appended to the aniline rather than in the quin(az)oline core.

Table 4. Matched pair comparison of benzyloxyaniline

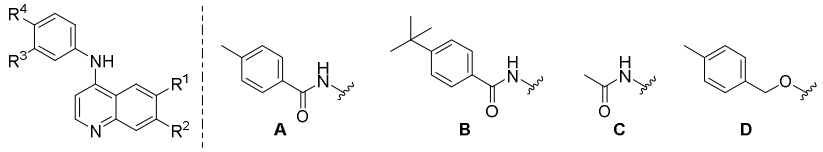

Compound	R^1	R^2	R^3	R^4	*Mtb* signal[a]				
					1.25 µM	2.5 µM	5 µM	10 µM	20 µM
29	OMe	OMe	OH	**A**	1.14	1.09	1.13	1.05	0.45
30	OMe	OMe	OH	**B**	1.10	1.12	1.06	0.72	0.25
31	OMe	OMe	H	**C**	1.21	1.10	1.11	1.07	1.02
32	OMe	H	OH	**A**	1.11	1.17	1.14	1.28	0.95
33	H	OMe	OH	**A**	1.13	1.11	1.09	1.11	0.96
34	OMe	OMe	H	**D**	0.43	0.17	0.10	0.08	0.09

[a]Relative luminescence was measured at 3 days after treatment. Values = RLU(sample)/RLU(no compound)

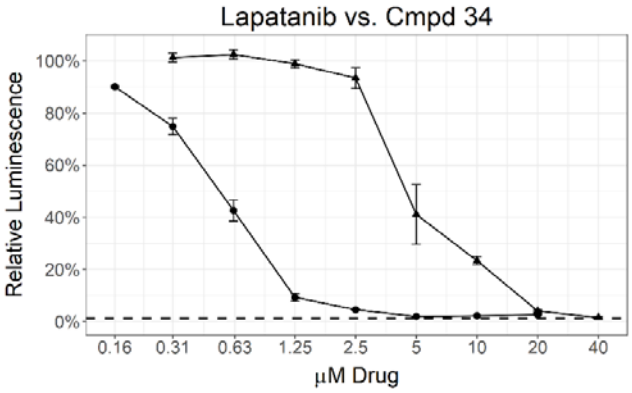

Figure 3. MIC determination by two different assays for **34** (circle) and lapatanib (triangle). Data points represent the mean of 3 biological replicates with standard deviation. The dashed line labeled 1% inoculum represents an inoculation of 1 % of the number of cells used for compound testing. This control was used to determine 99 % inhibition of growth.

This body of work provides a number of exciting starting points for further optimization. However, the failure to achieve complete parasite kill led us to deprioritize the series due to the potential for resistance to develop. The mechanism of anti-*Mtb* activity of these quin(az)olines has yet to be defined. These compounds were originally prepared as inhibitors of human kinases targeting the ATP-binding site, a rational starting hypothesis for the mechanism of action is that the effects of these compounds are mediated by inhibition of *Mtb* kinases. However, it is possible that the observed phenotypes may originate from modulation of other, non-kinase ATP-binding proteins in the organism.

Gefitinib, erlotinib, and lapatinib have previously been reported to inhibit the intracellular growth of *Mtb*. The authors provided multiple lines of evidence that inhibition of the host target epidermal growth factor receptor (EGFR) was responsible for this activity.[15] However our results suggest that there may be further targets involved, with the benzyl substituent presence in the molecule showing a pivotal effect to potency, as is highlighted by the activity of **30** vs **34**. The present results may help define a medicinal chemistry trajectory towards anti-tubercular compounds with targets in both the host and the parasite itself. Such dual acting compounds might offer advantages in efficacy and/or reduction in propensity for resistance.

Acknowledgments

The SGC is a registered charity (number 1097737) that receives funds from AbbVie, Bayer Pharma AG, Boehringer Ingelheim, Canada Foundation for Innovation, Eshelman Institute for Innovation, Genome Canada, Innovative Medi-cines Initiative (EU/EFPIA) [ULTRA-DD grant no. 115766], Janssen, Merck KGaA Darmstadt Germany, MSD, Novartis Pharma AG, Ontario Ministry of Economic Development and Innovation, Pfizer, São Paulo Research Foundation-FAPESP, Takeda, and Wellcome [106169/ZZ14/Z]. C. G. is supported by R01 AI117023 from the NIH/NIAID**.** We are grateful Dr. Brandie Ehrmann for LC-MS/HRMS support provided by the Mass Spectrometry Core Laboratory at the University of North Carolina at Chapel Hill.

References and notes

1. Pai, M.; Behr, M. A.; Dowdy, D.; Dheda, K.; Divangahi, M.; Boehme, C. C.; Ginsberg, A.; Swaminathan, S.; Spigelman, M.; Getahun, H.; Menzies, D.; Raviglione, M. *Nat Rev Dis Primers* **2016**, *2*, 16076.
2. World Health Organization. Global Tuberculosis Report 2018 (WHO, **2018**).
3. Chan, E. D.; Iseman, M. D. *BMJ.* **2002**, *325*, 1282.
4. Floyd, K.; Glaziou, P.; Zumla, A.; Raviglione, M. *Lancet Respir Med* **2018**, *6*, 299.
5. Ferguson, F. M.; Gray, N. S. *Nat Rev Drug Discov.* **2018**, *17*, 353.
6. Sachan, M.; Srivastava, A.; Ranjan. R.; Gupta, A.; Pandya, S.; Misra, A. *Curr Pharm Des.* **2016**, *22*, 2599.
7. Glennon, E. K. K.; Dankwa, S.; Smith, J. D.; Kaushansky, A. *Trends Parasitol.* **2018**, *34*, 843.
8. Drewry, D. H.; Wells, C. I.; Andrews, D. M.; Angell, R.; Al-Ali, H.; Axtman, A. D.; Capuzzi, S. J.; Elkins, J. M.; Ettmayer, P.; Frederiksen, M.; Gileadi, O.; Gray, N.; Hooper, A.; Knapp, S.; Laufer, S.; Luecking, U.; Michaelides, M.; Muller, S.; Muratov, E.; Denny, R. A.; Saikatendu, K. S.; Treiber, D. K.; Zuercher, W. J.; Willson, T. M. *PLoS One* **2017**, *12*, e0181585.
9. Elkins, J. M.; Fedele, V.; Szklarz, M.; Abdul Azeez, K. R.; Salah, E.; Mikolajczyk, J.; Romanov, S.; Sepetov, N.; Huang, X. P.; Roth, B. L.; Al Haj Zen, A.; Fourches, D.; Muratov, E.; Tropsha, A.; Morris, J.; Teicher, B. A.; Kunkel, M.; Polley, E.; Lackey, K. E.; Atkinson, F. L.; Overington, J. P.; Bamborough, P.; Muller, S.; Price, D. J.; Willson, T. M.; Drewry, D. H.; Knapp, S.; Zuercher, W. J. *Nat Biotechnol* **2016**, *34*, 95.
10. Asquith, C. R. M.; Laitinen, T.; Bennett, J. M.; Godoi, P. H.; East, M. P.; Tizzard, G. J.; Graves, L. M.; Johnson, G. L.; Dornsife, R. E.; Wells, C. I.; Elkins, J. M.; Willson, T. M.; Zuercher, W. J. *ChemMedChem* **2018**, 13, 48.
11. Derbyshire, E. R.; Zuzarte-Luís, V.; Magalhães, A. D.; Kato, N.; Sanschagrin, P. C.; Wang, J.; Zhou, W.; Miduturu, C. V.; Mazitschek, R.; Sliz, P.; Mota, M. M.; Gray, N. S.; Clardy, J. *Chembiochem.* **2014**, *15*, 1920.
12. Wlodarchak, N.; Teachout, N.; Beczkiewicz, J.; Procknow, R.; Schaenzer, A. J.; Satyshur, K.; Pavelka, M.; Zuercher, W.; Drewry, D.; Sauer, J. D.; Striker, R. *Mol Pharm.* **2018**, *15*, 5410.
13. Anastassiadis, T.; Deacon, S. W.; Devarajan, K.; Ma, H.; Peterson, J. R. *Nat Biotechnol.* **2011**, *29*, 1039.
14. Davis, M. I.; Hunt, J. P.; Herrgard, S.; Ciceri, P.; Wodicka, L. M.; Pallares, G.; Hocker, M.; Treiber, D. K.; Zarrinkar, P. P. *Nat Biotechnol.* **2011**, *29*, 1046.
15. Stanley, S. A.; Barczak, A. K.; Silvis, M. R.; Luo, S. S.; Sogi, K.; Vokes, M.; Bray, M. A.; Carpenter, A. E.; Moore, C. B.; Siddiqi, N.; Rubin, E. J.; Hung, D. T. *PLoS Pathog.* **2014**, *10*, e1003946.
16. Andreu, N.; Fletcher, T.; Krishnan, N.; Wiles, S.; Robertson, B. D. *J Antimicrob Chemother.* **2012**, *67*, 404.
17. An H37Rv strain containing an auto-luminescence operon (LuxABCDE) was grown to log phase, diluted and re-grown for at least 2 doublings to a final OD_{600} of 0.005. Cultures were dispensed into 96-well white, flat-bottom plates in 100 µL final volume. Luminescence was quantified using a PHERTAstar plate reader (BMG Labtech) blanked against 7H9 media.
18. Asquith, C. R. M.; Naegeli, K. M.; East, M. P.; Laitinen, T.; Havener, T. M.; Wells, C. I.; Johnson, G. L.; Drewry, D. H.; Zuercher, W. J.; Morris, D. C. pre-print *bioRxiv* **2018**, doi: https://doi.org/10.1101/475251.
19. **General procedure for the synthesis of 4-anilinoquin(az)olines**: 4-chloroquin(az)oline derivative (1.0 eq.), aniline derivative (1.1 eq.), and $^{i}Pr_2NEt$ (2.5 eq.) were suspended in ethanol (10 mL) and refluxed for 18 h. The crude mixture was purified by flash chromatography using EtOAc:hexane followed by 1-5 % methanol in EtOAc; After solvent removal under reduced pressure, the product was obtained as a free following solid or recrystallized from ethanol/water.
4-{[4-(benzyloxy)phenyl]amino}quinazolin-6-ol (**1**) as a yellow solid (68 %, 220 mg, 0.640 mmol) MP 231-233 °C; ^{1}H NMR (400 MHz, DMSO-d_6) δ 11.21 (s, 1H), 10.91 (s, 1H), 8.75 (s, 1H), 8.04 (d, *J* = 2.5 Hz, 1H), 7.88 (d, *J* = 9.0 Hz, 1H), 7.70 (dd, *J* = 9.1, 2.5 Hz, 1H), 7.62 – 7.57 (m, 2H), 7.52 – 7.44 (m, 2H), 7.44 – 7.37 (m, 2H), 7.37 – 7.30 (m, 1H), 7.14 – 7.09 (m, 2H), 5.16 (s, 2H). ^{13}C NMR (101 MHz, DMSO-d_6) δ 158.8, 157.8, 156.7, 148.1, 136.9, 131.6, 129.7, 128.5 (2C, s), 127.9, 127.7 (2C, s), 126.5, 126.2 (2C, s), 121.2, 114.92, 114.85 (2C, s), 107.1, 69.4. HRMS m/z $[M+H]^+$ calcd for $C_{21}H_{18}N_3O_2$: 344.1399 found = 344.1386; LC t_R = 4.24 min, >98% Purity.
4-{[4-(benzyloxy)phenyl]amino}quinazolin-7-ol (**2**) as a light yellow solid (78 %, 223 mg, 0.648 mmol) MP 277-279 °C; ^{1}H NMR (400 MHz, DMSO-d_6) δ 11.76 (s, 1H), 11.42 (s, 1H), 8.76 (d, *J* = 9.0 Hz, 1H), 8.74 (s, 1H), 7.59 – 7.54 (m, 2H), 7.49 – 7.44 (m, 2H), 7.42 – 7.38 (m, 2H), 7.36 – 7.28 (m, 3H), 7.12 – 7.07 (m, 2H), 5.15 (s, 2H). ^{13}C NMR (101 MHz, DMSO-d_6) δ 164.3, 158.9,

156.6, 150.5, 140.4, 136.9, 129.7, 128.5 (2C, s), 127.9, 127.7 (2C, s), 127.1, 126.3 (2C, s), 119.4, 114.8 (2C, s), 105.8, 102.0, 69.4. HRMS m/z $[M+H]^+$ calcd for $C_{21}H_{18}N_3O_2$: 344.1399 found = 344.1386; LC t_R = 4.33 min, >98% Purity.

4-{[4-(benzyloxy)phenyl]amino}quinazoline-6,7-diol (**3**) as a light yellow solid (69 %, 189 mg, 0.527 mmol) MP 272-274 ºC; ^{1}H NMR (400 MHz, DMSO-d_6) δ 10.32 (s, 2H), 8.53 (s, 1H), 7.91 (s, 1H), 7.64 – 7.53 (m, 2H), 7.50 – 7.44 (m, 2H), 7.43 – 7.37 (m, 2H), 7.36 – 7.30 (m, 2H), 7.20 (s, 1H), 7.10 – 7.01 (m, 2H), 5.13 (s, 2H). ^{13}C NMR (101 MHz, DMSO-d_6) δ 157.4, 155.7, 154.3, 149.1, 147.7, 137.1, 131.2, 128.5 (2C, s), 127.8, 127.7 (2C, s), 125.4 (2C, s), 114.7 (2C, s), 107.3, 106.7, 104.9, 69.4. HRMS m/z $[M+H]^+$ calcd for $C_{21}H_{18}N_3O_3$: 360.1348 found = 360.1335; LC t_R = 4.22 min, >98% Purity.

***N*-(4-(benzyloxy)phenyl)-6-methoxyquinazolin-4-amine** (**4**) as a light yellow solid (84 %, 231 mg, 0.647 mmol) MP 270-272 ºC; ^{1}H NMR (400 MHz, DMSO-d_6) δ 11.64 (s, 1H), 8.79 (s, 1H), 8.41 (d, *J* = 2.6 Hz, 1H), 7.92 (d, *J* = 9.1 Hz, 1H), 7.72 (dd, *J* = 9.2, 2.5 Hz, 1H), 7.68 – 7.53 (m, 2H), 7.53 – 7.18 (m, 5H), 7.18 – 7.04 (m, 2H), 5.17 (s, 2H), 4.00 (s, 3H). ^{13}C NMR (101 MHz, DMSO-d_6) δ 159.0 (2C, s), 156.8, 148.8, 136.9, 133.3, 129.6, 128.5 (2C, s), 127.9, 127.7 (2C, s), 126.8, 126.4 (2C, s), 121.4, 114.9 (2C, s), 114.6, 104.6, 69.4, 56.7. HRMS m/z $[M+H]^+$ calcd for $C_{22}H_{19}N_3O_2$: 357.1477 found = 358.1546; LC t_R = 4.53 min, >98% Purity.

***N*-[4-(benzyloxy)phenyl]-7-methoxyquinazolin-4-amine** (**5**) as a colourless solid (91 %, 251 mg, 0.701 mmol) MP 247-249 ºC; ^{1}H NMR (400 MHz, DMSO-d_6) δ 11.58 (s, 1H), 8.87 (d, *J* = 9.3 Hz, 1H), 8.81 (s, 1H), 7.71 – 7.57 (m, 2H), 7.58 – 7.12 (m, 7H), 7.13 – 6.99 (m, 2H), 5.15 (s, 2H), 3.97 (s, 3H). ^{13}C NMR (101 MHz, DMSO-d_6) δ 164.7, 158.9, 156.7, 150.8, 140.7, 136.9, 129.6, 128.5 (2C, s), 127.9, 127.7 (2C, s), 127.0, 126.3 (2C, s), 118.7, 114.8 (2C, s), 107.1, 100.1, 69.4, 56.3. HRMS m/z $[M+H]^+$ calcd for $C_{22}H_{19}N_3O_2$: 357.1477 found = 358.1547; LC t_R = 4.49 min, >98% Purity.

***N*-(4-(benzyloxy)phenyl)-6,7-dimethoxyquinazolin-4-amine** (**6**) as a colourless solid (84 %, 217 mg, 0.561 mmol) MP 250-252 ºC; ^{1}H NMR (400 MHz, DMSO-d_6) δ 11.44 (s, 1H), 8.73 (s, 1H), 8.36 (s, 1H), 7.68 – 7.56 (m, 2H), 7.55 – 7.43 (m, 2H), 7.43 – 7.15 (m, 4H), 7.15 – 7.03 (m, 2H), 5.15 (s, 2H), 4.00 (s, 3H), 3.96 (s, 3H). ^{13}C NMR (101 MHz, DMSO-d_6) δ 157.9, 156.5, 156.0, 150.0, 148.6, 137.0, 135.5, 129.9, 128.5 (2C, s), 127.9, 127.7 (2C, s), 126.3 (2C, s), 114.8 (2C, s), 107.1, 104.1, 99.8, 69.4, 57.0, 56.4. HRMS m/z $[M+H]^+$ calcd for $C_{23}H_{21}N_3O_3$: 388.1661 found = 388.1651; LC t_R = 4.55 min, >98% Purity.

4-{[4-(benzyloxy)phenyl]amino}quinolin-6-ol (**7**) as a light yellow solid (64 %, 182 mg, 0.532 mmol) MP 218-220 ºC; ^{1}H NMR (400 MHz, DMSO-d_6) δ 10.67 (s, 1H), 10.37 (s, 1H), 8.32 (d, *J* = 6.8 Hz, 1H), 7.96 (d, *J* = 9.1 Hz, 1H), 7.91 (d, *J* = 2.5 Hz, 1H), 7.63 (dd, *J* = 9.1, 2.4 Hz, 1H), 7.58 – 7.44 (m, 2H), 7.46 – 7.22 (m, 5H), 7.23 – 7.13 (m, 2H), 6.57 (d, *J* = 6.8 Hz, 1H), 5.17 (s, 2H). ^{13}C NMR (101 MHz, DMSO-d_6) δ 157.3, 156.5, 154.1, 140.1, 136.8, 132.2, 130.2, 128.5 (2C, s), 128.0, 127.8 (2C, s), 127.2 (2C, s), 124.9, 121.9, 118.7, 116.0 (2C, s), 105.4, 98.6, 69.5. HRMS m/z $[M+H]^+$ calcd for $C_{22}H_{19}N_2O_2$: 343.1447 found = 343.1433; LC t_R = 4.45 min, >98% Purity.

4-({4-[(4-fluorophenyl)methoxy]phenyl}amino)quinazolin-6-ol (**8**) as a yellow solid (76 %, 228 mg, 0.631 mmol) Decomposed >200 ºC; ^{1}H NMR (400 MHz, DMSO-d_6) δ 11.22 (s, 1H), 10.91 (s, 1H), 8.75 (s, 1H), 8.05 (d, *J* = 2.5 Hz, 1H), 7.88 (d, *J* = 9.0 Hz, 1H), 7.70 (dd, *J* = 9.0, 2.4 Hz, 1H), 7.67 – 7.54 (m, 2H), 7.57 – 7.39 (m, 2H), 7.40 – 7.17 (m, 2H), 7.17 – 7.01 (m, 2H), 5.14 (s, 2H). ^{13}C NMR (101 MHz, DMSO-d_6) δ 163.0, 159.7 (d, *J* = 175.5 Hz), 157.8, 156.6, 148.1, 133.2 (d, *J* = 3.0 Hz), 131.6, 130.0 (d, *J* = 8.3 Hz, 2C), 129.8, 126.5, 126.2 (2C, s), 121.2 115.3 (d, *J* = 21.4 Hz, 2C), 114.93, 114.86 (2C, s), 107.1, 68.7. HRMS m/z $[M+H]^+$ calcd for $C_{21}H_{17}N_3O_2F$: 362.1305 found = 362.1290; LC t_R = 4.31 min, >98% Purity.

4-({4-[(3-fluorophenyl)methoxy]phenyl}amino)quinazolin-6-ol (**9**) as a dark green solid (58 %, 174 mg, 0.482 mmol) 138-140 ºC; ^{1}H NMR (400 MHz, DMSO-d_6) δ 11.25 (s, 1H), 10.94 (s, 1H), 8.74 (s, 1H), 8.06 (d, *J* = 2.5 Hz, 1H), 7.89 (d, *J* = 9.0 Hz, 1H), 7.71 (dd, *J* = 9.0, 2.4 Hz, 1H), 7.67 – 7.49 (m, 2H), 7.45 (td, *J* = 8.0, 6.0 Hz, 1H), 7.41 – 7.22 (m, 2H), 7.21 – 6.93 (m, 3H), 5.19 (s, 2H). ^{13}C NMR (101 MHz, DMSO-d_6) δ 162.20 (d, *J* = 243.7 Hz), 158.83, 157.80, 156.43, 148.07, 139.93 (d, *J* = 7.4 Hz), 131.62, 130.52 (d, *J* = 8.4 Hz), 129.89, 126.48, 126.26 (2C, s), 123.54 (d, *J* = 2.8 Hz), 121.14, 114.93, 114.87 (2C, s) , 114.63 (d, *J* = 20.9 Hz), 114.23 (d, *J* = 21.9 Hz), 107.13, 68.57 (d, *J* = 1.9 Hz). HRMS m/z $[M+H]^+$ calcd for $C_{21}H_{17}N_3O_2F$: 362.1305 found = 362.1296; LC t_R = 4.25 min, >98% Purity.

4-({4-[(2-fluorophenyl)methoxy]phenyl}amino)quinazolin-6-ol (**10**) as a dark green solid (69 %, 207 mg, 0.573 mmol) 235-237 ºC; ^{1}H NMR (400 MHz, DMSO-d_6) δ 11.23 (s, 1H), 10.91 (s, 1H), 8.75 (s, 1H), 8.05 (d, *J* = 2.5 Hz, 1H), 7.88 (d, *J* = 9.0 Hz, 1H), 7.70 (dd, *J* = 9.0, 2.4 Hz, 1H), 7.66 – 7.48 (m, 3H), 7.48 – 7.38 (m, 1H), 7.38 – 7.19 (m, 2H), 7.19 – 7.05 (m, 2H), 5.19 (s, 2H). ^{13}C NMR (101 MHz, DMSO-d_6) 160.4 (d, *J* = 246.1 Hz), 158.8, 157.8, 156.5, 148.1, 131.7, 130.7 (d, *J* = 4.1 Hz), 130.5 (d, *J* = 8.3 Hz), 129.9, 126.5, 126.3 (2C, s), 124.6 (d, *J* = 3.5 Hz), 123.7 (d, *J* = 14.5 Hz), 121.2, 115.4 (d, *J* = 21.0 Hz), 114.9, 114.8 (2C, s), 107.1, 63.8 (d, *J* = 3.7 Hz). HRMS m/z $[M+H]^+$ calcd for $C_{21}H_{17}N_3O_2F$: 362.1305 found = 362.1291; LC t_R = 4.30 min, >98% Purity.

4-((4-((4-fluorobenzyl)oxy)phenyl)amino)quinazolin-7-ol (**11**) as a grey solid (58 %, 174 mg, 0.482 mmol) Decomposed >300 ºC; ^{1}H NMR (400 MHz, DMSO-d_6) δ 11.74 (s, 1H), 11.38 (s, 1H), 8.81 – 8.66 (m, 2H), 7.66 – 7.38 (m, 4H), 7.29 (dd, *J* = 6.9, 2.4 Hz, 2H), 7.27 – 7.15 (m, 2H), 7.14 – 7.05 (m, 2H), 5.13 (s, 2H). ^{13}C NMR (101 MHz, DMSO-d_6) δ 164.2, 161.8 (d, *J* = 243.7 Hz), 158.9, 156.5, 150.5, 140.5, 133.2 (d, *J* = 3.0 Hz), 130.0 (d, *J* = 8.3 Hz, 2C), 129.7, 127.1, 126.3 (2C, s), 119.4, 115.3 (d, *J* = 21.4 Hz, 2C), 114.8 (2C, s), 105.8, 102.1, 68.7. HRMS m/z $[M+H]^+$ calcd for $C_{21}H_{17}N_3O_2F$: 362.1305 found = 362.1291; LC t_R = 4.44 min, >98% Purity.

4-((4-((4-fluorobenzyl)oxy)phenyl)amino)quinazoline-6,7-diol (**12**) as a colourless solid (55 %, 158 mg, 0.420 mmol) 285-290 ºC; ^{1}H NMR (400 MHz, DMSO-d_6) δ 10.34 (s, 1H), 8.55 (s, 1H), 7.88 (s, 1H), 7.70 – 7.35 (m, 4H), 7.33 – 7.12 (m, 3H), 7.12 – 7.01 (m, 2H), 5.12 (s, 2H). ^{13}C NMR (126 MHz, DMSO-d_6) δ 161.8 (d, *J* = 243.5 Hz), 157.4, 155.7, 154.4, 149.0, 147.7, 137.4, 133.3 (d, *J* = 8.3 Hz, 2C), 130.9, 130.0 (d, *J* = 8.4 Hz, 2C), 125.4, 115.3 (d, *J* = 21.3 Hz, 2C), 114.8 (s, 2C), 107.2, 106.8, 104.6, 68.7. HRMS m/z $[M+H]^+$ calcd for $C_{21}H_{17}N_3O_3F$: 378.1254 found = 378.1240; LC t_R = 4.29 min, >98% Purity.

20. Compounds **13-28** prepared as previously described.[10]
21. Compounds **29-34** prepared as previously described.[22]
22. Asquith, C. R. M.; Maffuid, K. A.; Laitinen, T.; Torrice, C. D.; Tizzard, G. J.; Koshlap, K. M.; Crona, D. J.; Zuercher, W. J. Preprint *bioRxiv* **2019**, doi: https://doi.org/10.1101/545525

Supplementary Material

Supplementary material